

1

2

Relation between concentration and shear-extensional rheology properties of xanthan and guar gum solutions

3

4

5

6

J.E. Martín-Alfonso^{a,*}, A.A. Cuadri^a, M. Berta^b, M. Stading^{b,c}

7

^a Department of Chemical Engineering and Material Science, Campus de El Carmen,
University of Huelva, Chemical Product and Process Technology Research Center
(Pro2TecS). 21071 Huelva. Spain.

8

9

10

^b Research Institutes of Sweden, Bioscience and Materials, Product Design and
Perception, 402 29 Gothenburg, Sweden .

11

12

^c Chalmers University of Technology, Department of Industrial and Materials Science,
412 96 Gothenburg, Sweden.

13

14

15

* Corresponding author. Tel.: +34 9599985; fax: +34 959219385.

16

E-mail addresses: jose.martin@diq.uhu.es (J.E. Martín-Alfonso)

17

18

19 ABSTRACT

20 The influence of concentration on the shear and extensional rheology properties of
21 aqueous solutions of xanthan and guar gums was studied in this work. Shear rheology
22 involved small amplitude oscillatory shear (SAOS), flow curves and transient flow,
23 while the extensional rheology was analyzed using hyperbolic contraction flow. In
24 addition, the mechanical properties during solutions manufacture were monitored in situ
25 through the evolution of torque with processing time by mixing rheometry. The results
26 showed that the hydrocolloids exert a great influence on the process rheokinetics and on
27 the resulting rheological response. SAOS tests showed that the xanthan gum solutions
28 behaved as weak gels, whereas guar gum solutions suggest the presence of
29 entanglement and the formation of a viscoelastic, gel-like structure. All the systems
30 exhibited shear-thinning behaviour. Guar gum solutions obeyed the Cox-Merz rule,
31 with some divergence at high rates for the more concentrated solutions, while the Cox-
32 Merz rule was not followed for xanthan gum in the range of concentration studied. The
33 extensional viscosity exhibited an extensional-thinning behaviour within the strain
34 range used and all solutions were characterized by a high Trouton ratio.

35

36 *Keywords:* Polysaccharides solutions; Viscoelasticity; Flow behaviour; Shear thickening

37

38 **1. Introduction**

39 Nowadays, polysaccharides play a leading role as large source of biomass based
40 materials useful for various applications (Lapasin & Pricl, 1995). They can be processed
41 in different ways and their ability to form solutions and gels under specific conditions is
42 the basis for important applications within areas such as cosmetic, biomedical,
43 pharmaceutical and food technology (Tombs & Harding, 1998). The rheological
44 properties of these materials depend on the nature of its components and the molecular
45 interactions between the polymer and solvent, in the product and during its processing.
46 Hence, it is possible to obtain novel products by proper selection of the ingredients, but
47 also by process optimization. Guar gum (GG) is a water-soluble galactomannan from
48 the endosperm portion of the guar bean (*Cyamopsis tetragonoloba*) (Mudgil, Barak, &
49 Khatkar, 2012; Szopinski, & Luinstra, 2016). Guar gum molecule has a backbone
50 composed of a linear chain of β -1,4-linked mannose units with randomly attached α -
51 1,6-linked galactose units. The mannose-to-galactose ratio in guar gum ranges from 1.6
52 and 1.8, varying with the source (Cheng, & Prud'homme, 2000) and this ratio is
53 important in determining the mechanical properties of the solutions (Sittikijyothin,
54 Torres, & Gonçalves, 2005). It can be utilized as stabilizing and thickening agent to
55 form solutions in a broad range of concentrations in several industries such as food,
56 agriculture, cosmetics, textile etc. (Miquelim, & Lannes, 2009). It has been extensively
57 used in a range of applications because of its unique ability to produce viscous solutions
58 with tuneable mechanical properties. Xanthan gum (XG) is a polysaccharide secreted by
59 *Xanthomonas campestris* and composed of a (1 \rightarrow 4) linked β -D-glucan (cellulose)
60 backbone that is substituted on the O-3 position of alternating glucose residues by
61 charged trisaccharide side chains of β -D-mannospyranosyl-(1 \rightarrow 4)- β -D-
62 glucuronopyranosyl-(1 \rightarrow 2)-6-O-acetyl- β -D-mannospyranosyl (Choi, & Yoo, 2009;

63 Sworn, 2000). Xanthan gum is soluble in hot or cold water, and solutions exhibit a large
64 increase in the viscosity at low concentrations, and exhibit a pronounced shear-thinning
65 behaviour. Commonly used as a food thickening agent and a stabilizer and due to its
66 rheological properties it has been utilized in a wide range of industrial applications
67 (Sworn, 2000). The rheological properties of guar and xanthan gum solutions are useful
68 to understand the polysaccharide structure and to investigate its potential functionalities
69 in a wide range of engineering applications. Traditionally, the rheological properties of
70 guar and xanthan gum aqueous solutions have been determined through flow curves and
71 small amplitude oscillatory shear (Tako, & Nakamura, 1985; Abdulrahman, Alquraishi,
72 & Fares Alsewailem, 2012). In recent years, extensional rheology has received
73 increasing attention since it is crucial for many polymer processing operations,
74 consumer perception and product quality and due to experimental techniques have
75 evolved and become widely available. For instance, industrial applications often involve
76 extensional flow in addition to shear flow. In some cases, the extensional deformation
77 dominates, as it is the case of a flow through a contraction, or a melt stretched during
78 film blowing or between rotating rollers (Piermaría, Bengoechea, Abraham, &
79 Guerrero, 2016). Studies have shown that a food bolus is subject to both shear and
80 extensional flow during mastication when the bolus is compressed between the tongue
81 and the soft palate (Hasegawa, Otaguro, Kumagai, & Nakazawa, 2005; Salinas-
82 Vázquez, et al., 2014), and that fluid elasticity contributes to safe swallowing (Nyström,
83 et al., 2015). Different experimental methods have been employed for quantifying the
84 extensional viscosity. Techniques for elongation of melts was developed early by
85 Meissner (1972) and Münstedt (1979) (Meissner, 1972; Münstedt, 1979). Filament
86 Stretching is a well-established laboratory technique (Sridhar, Tirtaatmadja, Nguyen, &
87 Gupta, 1991; Bach, Rasmussen, & Hassager, 2003), and the similar technique of
88 Capillary Breakup (CABER) is commercially available (Entov, & Yarin, 1984; Anna, &

89 McKinley, 2001). A spinline measurements can also be used to obtain qualitative
90 extensional data, and the material in form of a fibre, is then drawn with a drum and the
91 drawn profile of the material is captured by a camera. The required tensile force is
92 measured and together with the captured shape the extensional viscosity can be
93 evaluated. Furthermore, contraction flows exerts extensional stress in a fluid and by
94 pushing it through a hyperbolic nozzle designed to give a constant extension rate and
95 measuring the required pressure drop the extensional behaviour can be determined.
96 Hyperbolic Contraction Flow is the method used in the present work and it has been
97 used successfully for many systems such as suspensions (Moberg, Rigdahl, Stading, &
98 Bragd, 2014), dough/dairy products (Berta, Gmoser, Krona, & Stading, 2015),
99 commercial thickeners (Qazi, et al., 2017), food systems (Berta, Muskens, Schuster, &
100 Stading, 2016; Berta, Wiklund, Kotz, & Stading, 2016; Oom, Pettersson, Taylor, &
101 Stading, 2008) and polymer melts (Köpplmayr, et al., 2016). The advantages of this
102 technique are that it can create a controlled extensional flow and is suitable for medium-
103 viscosity fluids where melt elongation techniques or capillary breakup are not suitable.
104 Therefore, the objective of this work was to study the influence of concentration on the
105 shear and extensional rheology properties of aqueous solutions of xanthan and guar
106 gum. This rheological study involves small amplitude oscillatory shear (SAOS), steady
107 shear flow and transient flow. The extensional rheology determined in order to improve
108 the understanding of the rheological behaviour of these solutions in extensional flow to
109 allow them to be used more efficiently.

110 **2. Experimental**

111 *2.1. Materials and sample preparation*

112 Food grade powders of xanthan (X, Danisco, Sweden) and guar (G, Sigma-Aldrich,
113 India) were used as the gelling agent. Aqueous solutions of xanthan and guar gums at

114 concentrations of 1, 1.5 and 2 wt.% were prepared in distilled water by stirring at 900
115 rpm on a magnetic stirrer for 4 h at room temperature (20 - 23°C). Finally, the solutions
116 to be studied were left to stand for overnight at 4°C for complete hydration of the
117 biopolymer and removal of the remaining bubbles. Sodium azide was added to the
118 solution to prevent the growth of microorganisms.

119 *2.2. Rheological characterization*

120 *2.2.1 Shear rheology*

121 Rheological measurements were carried out in controlled-strain rheometer (ARES-G2,
122 TA Instruments, New Castle, USA), using a parallel plate geometry (40 mm diameter, 1
123 mm gap). Small-amplitude oscillatory shear (SAOS) measurements, inside the linear
124 viscoelasticity regime, were performed in a frequency range between 10^{-2} and 10^2 rad/s.
125 Strain sweep tests, at a frequency of 6.23 rad/s, were first performed to determine the
126 linear viscoelastic regime. Flow curves in shear flow were measured in the range 10^{-2} to
127 100 s^{-1} , according to a step-ramp of increasing shear rates (Torres, Hallmark, & Wilson,
128 2014). Viscosity was calculated in each step after a maximum shear time of 300 s,
129 unless the steady-state response had been previously achieved within 1% tolerance.
130 Transient shear stress experiments were performed at different constant shear rates
131 (0.01, 0.1, 1, 10 and 50 s^{-1}). The shear stress evolution was monitored until steady-state
132 was reached. In order to ensure accurate results, at least three replicates were conducted
133 for every sample/test. Figures present the average values \pm one standard deviation (SD).
134 The upper plate rim was covered with a thin layer of mineral oil (Dow Corning 200, 20
135 cSt) to prevent water evaporation. In addition, in situ torque measurements during the
136 polysaccharide solutions were monitored using a rheomixer experimental setup in order
137 to follow the solution efficiency. The device setup consisting of a cup (40 mm diameter,
138 71 mm height) and a stirring arrangement (four-blade mixing head, 30 mm diameter)

139 coupled with the transducer of a controlled-stress Haake RS600 rheometer (Germany).
140 This tool, successfully used in mixing applications (Martín-Alfonso, & Franco, (2014),
141 allows on-line monitoring of the evolution of torque with time, thus studying the
142 kinetics of the mixing process.

143 *2.2.2 Extensional rheology*

144 Extensional viscosity was measured using a Hyperbolic Contraction Flow rig (Nystrom,
145 2015; Stading, & Bohlin, 2001) mounted on an Instron 5542 Universal Testing
146 Instrument (Instron Corporation, Canton, MA, USA). Measurements were performed at
147 room temperature using a die with inlet radius of 15 mm and outlet radius of 1 mm,
148 imposing a total Hencky strain of 7.7 to the samples. The extensional strain rates were
149 in the same range of continuous shear flow measurements, $0.5\text{-}30\text{ s}^{-1}$, and the data was
150 evaluated as described previously (Nystrom, 2015; Binding, 1988). The transient
151 extensional stress was monitored until a stable plateau value was reached from which
152 the steady-state, and the transient extensional viscosity was calculated as described by
153 Wikstrom and Bohlin (1999). The Power-law parameters acquired with the continuous
154 shear measurements were used to calculate the extension rates, the Hencky strain and to
155 compensate for the shear stress contribution to the total stress (Wikstrom, & Bohlin,
156 1999). At least two replicates were performed on fresh samples.

157 **3. Results and discussion**

158 *3.1. Rheological properties during processing and linear viscoelasticity*

159 In order to study the influence of gum concentration on the rheological properties of
160 solutions and the evolution of the degree of solution of the gum in the water, different
161 samples with 1, 1.5 and 2 wt.% gum concentration were processed. **Fig. 1** shows the
162 evolution of torque during processing of solutions prepared in the Rheomixer as a
163 function of gum concentration. Attending to the evolution of torque, the system to form

164 a physically stable solutions may be divided in different steps. The first monitored
165 torque values correspond to those obtained just agitating the solvent (stage 1). When
166 gum was added, a sudden increase in torque was noticed and then still increase more
167 gradually as hydrocolloids were being intimately dispersed in the solvent (stage 2).
168 Finally, once the polysaccharide was totally well dispersed, torque tends to constant
169 values (stage 3). At this time, the mixing process was considered to be finished. The
170 experimental torque value with time was successfully fitted to the following equation:

$$171 \quad \frac{M - M_{\infty}}{M_0 - M_{\infty}} = \frac{1}{1 + \left(\frac{t}{t_{1/2}} \right)^p} \quad (1)$$

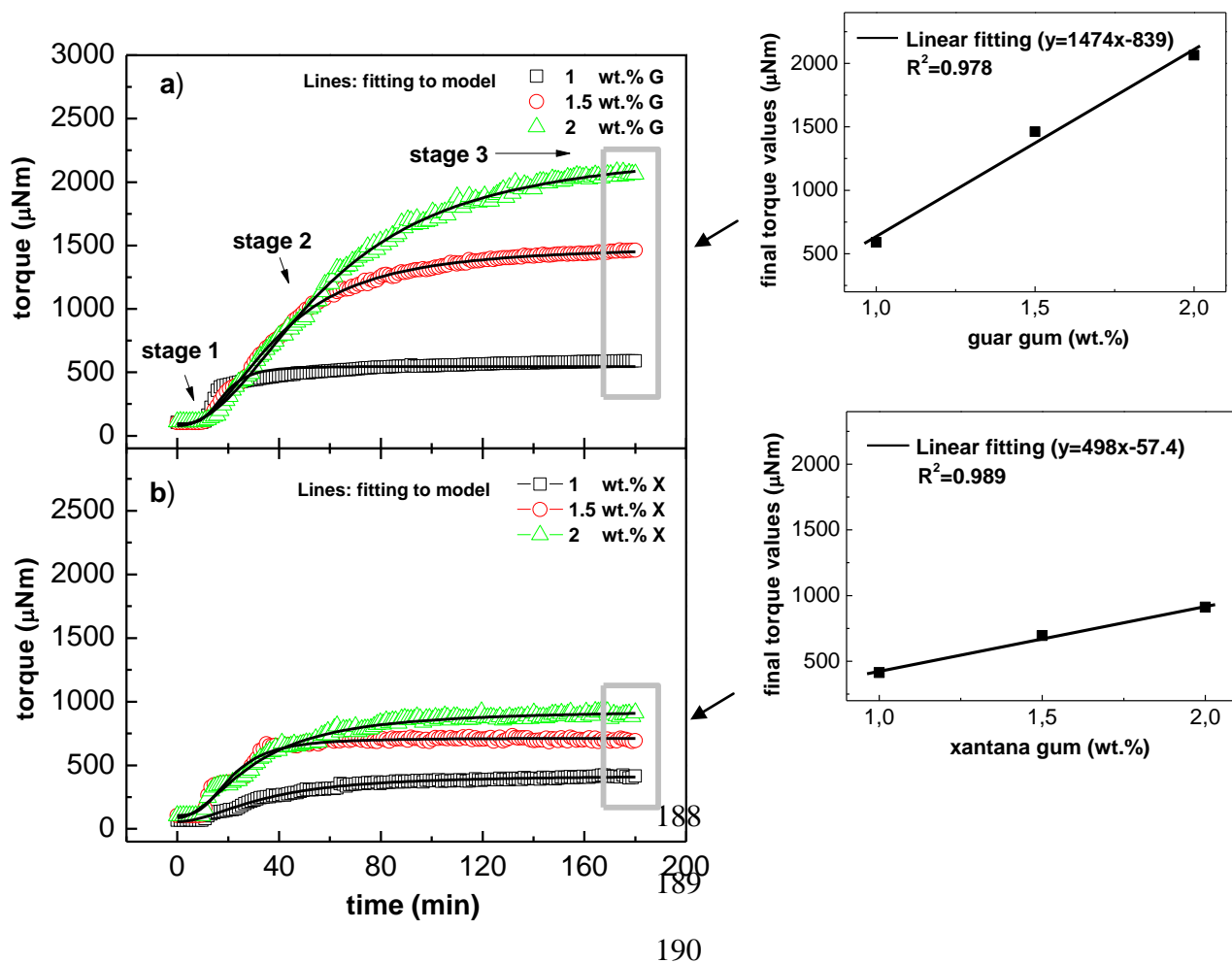
172 where M_0 and M_{∞} are the torque values right after the polysaccharide addition and at the
173 final step of the process, respectively, $t_{1/2}$ is the time necessary to reach an increase in
174 torque of 50% after the polysaccharide addition, and 'p' is a parameter related to the
175 slope of the rheokinetic curve. The values of fitting parameters are shown in **Table 1**. It
176 can be observed that both lower 'p' and higher $t_{1/2}$ values were obtained with increasing
177 polysaccharide concentration. Interestingly, the increase in torque values was more
178 gradual when dispersing guar gum, thus yielding higher $t_{1/2}$ values. Hence, these results
179 may shed light that the type of hydrocolloids exerts a great influence on the rheokinetic
180 process. Finally, as could be expected, an increased hydrocolloid concentration produce
181 an increase the torque values. The final torque values linearly increase with
182 hydrocolloid content as can be observed in the graph alongside in **Fig. 1**.

183

184

185

186



191 **Fig. 1.** Evolution of torque with time during processing of solutions as function of gum
 192 concentrations: a) guar, b) xanthan. The experimental data is fitted to Eq. (1).

193 **Table 1**

194 Fitting parameters corresponding to equation (4), for solutions manufactured in the
 195 'rheomixer'.

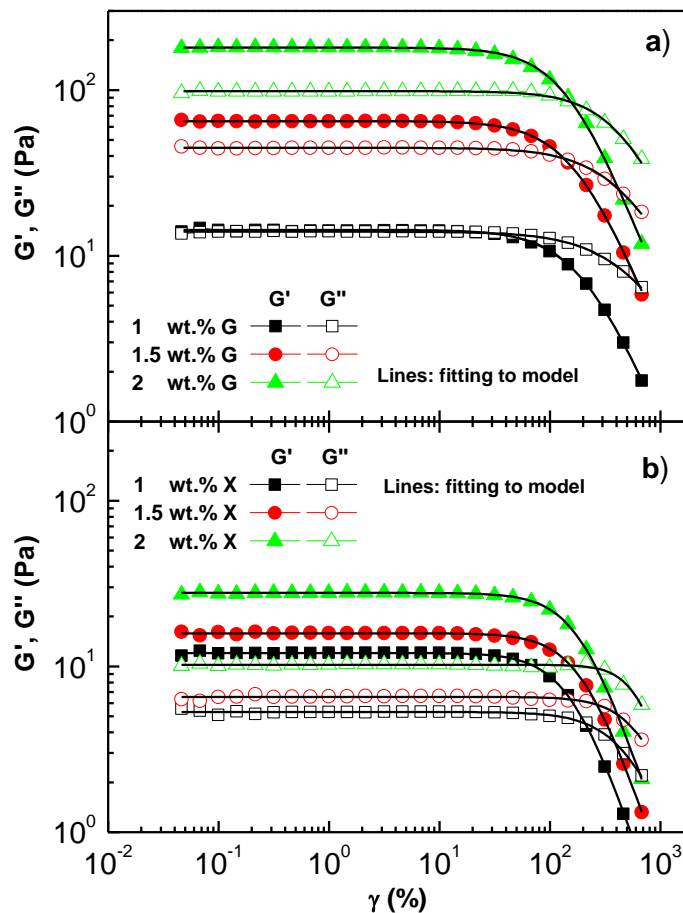
196

Sample	M_0 (μNm)	M_∞ (μNm)	$t_{1/2}$ (s)	p	R^2
1 wt.% guar	95.2±3.41	546.4±4.26	18.3±0.40	3.86±0.02	0.988
2 wt.% guar	79.6±4.73	1495.5±3.73	39.8±0.20	2.25±0.02	0.997
3 wt.% guar	86.1±8.61	2279.3±14.3	58.7±0.46	2.07±0.03	0.998
1 wt.% xanthan	57.2±3.06	423.5±2.36	34.7±0.46	1.88±0.05	0.994
2 wt.% xanthan	105.6±10.08	712.7±3.18	21.3±0.47	2.89±0.14	0.986
3 wt.% xanthan	86.5±9.88	935.9±6.38	30.4±0.56	1.92±0.06	0.991

197 Solutions were studied under oscillatory shear conditions, in order to define the upper
198 limit of the linear viscoelastic range (LVR) and determine the mechanical spectrum for
199 each sample. **Fig. 2** shows storage and loss moduli dependence on strain amplitude. As
200 long as the strain amplitude is small, G' and G'' curves present a constant plateau value.
201 Here, the structure of the sample is only slightly perturbed, with it is viscoelastic
202 response within the linear region (LVR) until a certain critical value (γ_c). This transition
203 from the linear to the non-linear viscoelastic regimes may be described by the Soskey–
204 Winter equation, applied to the both moduli, values ($r^2 > 0.995$):

$$205 \quad \frac{G}{G_0} = \frac{1}{1 + b\gamma^n} \quad (2)$$

206 where G_0 represents the limiting values of the modulus (G' or G'') in the linear
207 viscoelastic regime, γ is the strain and b and n are adjustable parameters. The critical
208 strain value γ_c marking the upper limit of the linear viscoelastic regime was arbitrarily
209 set in correspondence with $G/G_0=0.95$. It is worth noting that G' was clearly more
210 sensitive than G'' in the detection of the onset of nonlinear viscoelastic response. As
211 expected, both moduli increase with increasing polysaccharide concentration, consistent
212 with an increasing degree of association among macromolecules. Critical strain does
213 change significantly with polysaccharide concentration, since its value is generally
214 between 14 and 99%. As shown in **Fig. 2**, xanthan gum solutions show a somewhat
215 longer LVR compared to guar, indicating the network is less prone to yielding.

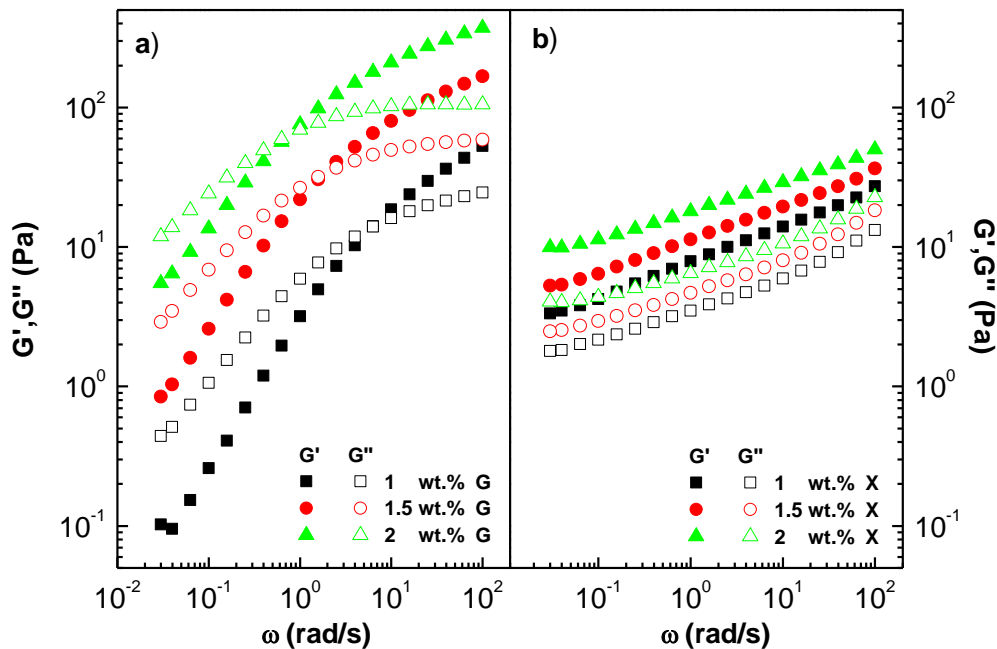


216

217 **Fig. 2.** Storage (G') and loss (G'') moduli as a function of strain for gum solutions with
 218 different concentrations: a) guar, b) xanthan.

219 **Fig. 3** shows the mechanical spectra (G' and G'' vs. angular frequency) of guar and
 220 xanthan aqueous solutions. Storage and loss moduli values (G' and G'') of the guar gum
 221 solutions (**Fig. 3a**) increased with angular frequencies and concentration, as expected.
 222 At low angular frequency the viscous component is dominant, but the increase on G''
 223 with frequency increased is lower than the increase on G' . Therefore, a crossover point
 224 at a characteristic frequency of the polymer at concentrations and two regions dependent
 225 on concentration were observed, being the region at high frequencies shorter as
 226 concentration decreased. The crossover frequency point is an indication of the inverse
 227 of the polymer solution relaxation time and decreased from 6.3 rad/s to 1 rad/s as the
 228 concentration increased from 1 wt.% to 2 wt.%. This behaviour is typical of low

229 concentrated macromolecular solutions showing an apparent fluid character with a
 230 tendency to a crossover in the high frequency regime. Similar results were founded by
 231 Chenlo, Moreira, & Silva, (2010). On the other hand, the mechanical behaviour of
 232 xanthan gum solutions is reported in **Fig. 3b**. The linear viscoelasticity response is
 233 qualitatively similar for all the solutions studied, where the storage modulus G' remains
 234 higher than the loss modulus G'' ($G' > G''$), which means that the elastic response is
 235 consequently higher than the viscosity response. Values between of 0.20 to 0.25 were
 236 obtained for the slope of all the G' vs. ω curves. Hence, the solutions studied exhibited
 237 weak-gel viscoelastic behaviour as demonstrated by this slope value and by the fact that
 238 G' values lay above those of G'' . These results were consistent with those previously
 239 reported for xanthan gum solutions (Choi et al., 2014; Carmona, Ramírez, Calero, &
 240 Muñoz, 2014; Choppe, Puaud, Nicolai, & Benyahia, 2010).



241

242 **Fig. 3.** Frequency dependence of the storage (G') and loss moduli (G''), in the linear
 243 viscoelasticity region, for aqueous gum solutions as a function of gum content.

244 3.2. Flow behaviour

245 Flow curves for guar gum solutions as function of concentration are shown in the form
246 of flow curves in **Fig. 4a**. The apparent viscosity at each shear rate increases noticeably
247 with polymer concentration. In all cases, the solutions exhibit shear thinning behavior at
248 rates $>10^{-1}$ while at a lower rate the curves approach the Newtonian plateau. These
249 experimental data were fitted by the Cross model ($R^2 > 0.998$).

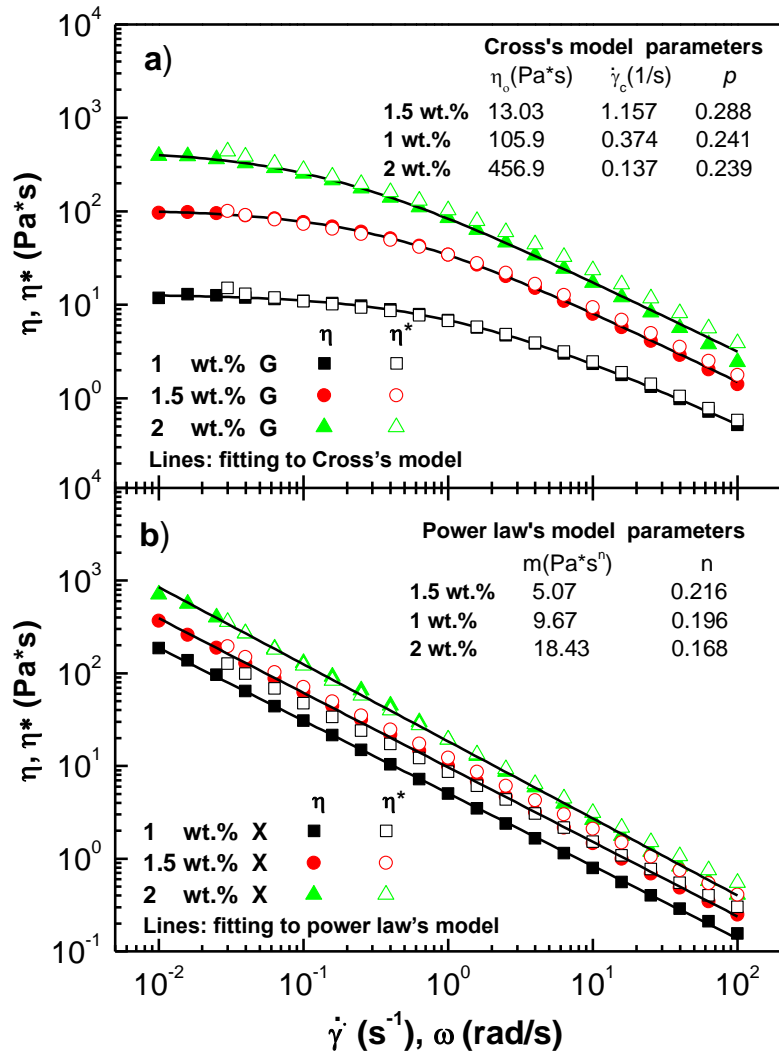
250

$$\eta = \frac{\eta_0}{\left(1 + \frac{\dot{\gamma}}{\dot{\gamma}_c}\right)^{1-p}} \quad (3)$$

251 where η_0 is the low-shear Newtonian viscosity, $\dot{\gamma}_c$ is the critical shear rate for the onset
252 of shear-thinning response and p is a parameter related to the slope of the power-law
253 region. The values of these parameters are shown in **Fig. 4a**. The η_0 values increased
254 significantly with increasing gum concentration, while $\dot{\gamma}_c$ values gradually decrease
255 with the concentration and the values of the slope, p , were quite similar. The variation
256 in η_0 and $\dot{\gamma}_c$ values confirms the effect of the concentration on both the viscosity at low
257 frequencies and the beginning of the shear thinning region. The increase of η_0 with
258 polymer concentration indicates the establishment of a greater number of links between
259 the biopolymer molecules and depends on the molar mass and on interchain
260 interactions. These results were consistent with those previously found for other guar
261 gum solutions (Torres, Hallmark, & Wilson, 2014; Duxenneuner, Fischer, Windhab, &
262 Cooper-White, 2008). Xanthan gum solutions showed shear thinning behavior without
263 any indication of a Newtonian plateau for $\dot{\gamma}_{>0.01}$ and were better fitted by the Ostwad-de
264 Waele Power law in the shear rate range studied ($R^2 > 0.995$):

265
$$\eta = m\dot{\gamma}^{n-1} \quad (4)$$

266 where “m” is a parameter related to the consistency of the sample and “n” is the slope of
267 the shear thinning region. The fitted parameters are shown in **Fig. 4b**. Values of the
268 consistency index clearly increases with xanthan gum concentrations, while the values
269 of the flow index gradually decrease with the concentration showing that shear thinning
270 is induced by the presence of xanthan gum in solution. In addition, **Fig. 4** provides a
271 comparison between complex viscosity, derived from SAOS measurements and steady
272 shear viscosity. As can be observed, guar gum solutions obeyed the Cox-Merz rule
273 (Cox, & Merz, 1958), $|\eta^*(\omega)| \approx \eta(\dot{\gamma})$ where $\omega = \dot{\gamma}$, relating the apparent viscosity
274 (steady shear flow) and the magnitude of the complex viscosity (oscillatory shear flow)
275 at a given frequency and shear rate. There is a divergence in behaviour at high rates for
276 the more concentrated solutions, probably due to entanglements. The deviation is
277 related to the elastic gel-like structure, which is not affected during oscillatory
278 measurements, but is broken during steady shear tests such that the measured magnitude
279 of the complex viscosity is larger than the apparent viscosity. Similar behaviour has
280 been reported by Torres et al. (2014), who also found that the largest deviations
281 occurred at higher angular frequencies and shear rates. On the other hand, the Cox-Merz
282 rule was not followed throughout the xanthan gum concentrations studied. The
283 departure from Cox-Merz rule confirms the occurrence of a structured system,
284 supporting that the weak-gel structure was clearly set. These results were consistent
285 with those previously reported (Carmona, et al., 2015).



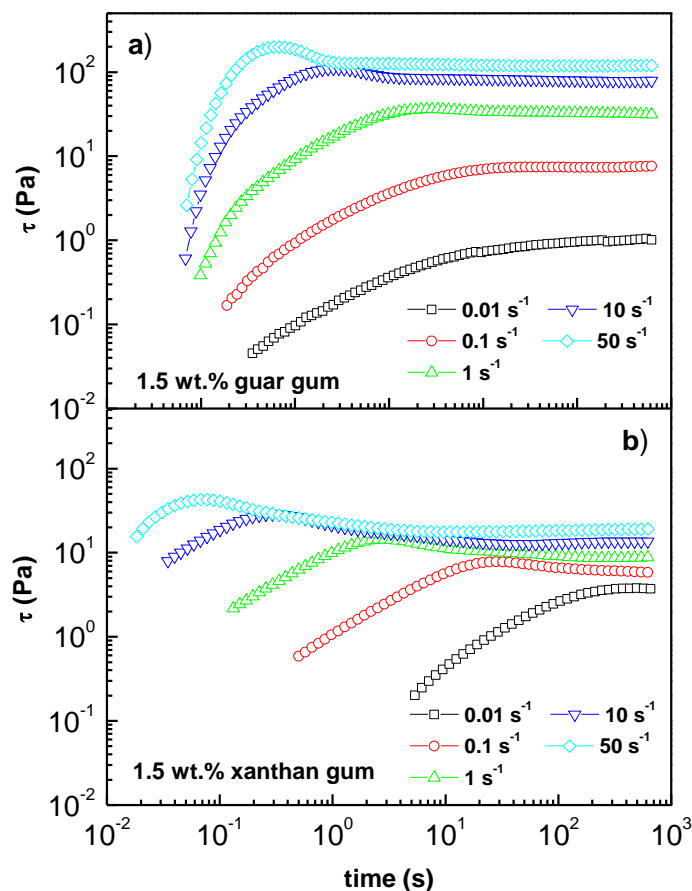
286

287 **Fig. 4.** Comparison between steady-state and complex viscosities for aqueous gum
 288 solutions.

289 *3.3. Transient flow*

290 **Fig. 5** shows selected shear stress vs. shear time plots for aqueous gum solutions
 291 containing 1.5% wt. gum at several constant shear rates. In all cases, a non-linear
 292 viscoelastic response was observed with two distinct regions: the first one comprised
 293 between the onset of the transient test and the maximum shear stress, the so-called stress
 294 overshoot (τ_{max}), and the second one ranging between this maximum and the
 295 equilibrium or steady-state shear stress (τ_{eq}). The shear-induced structural modifications

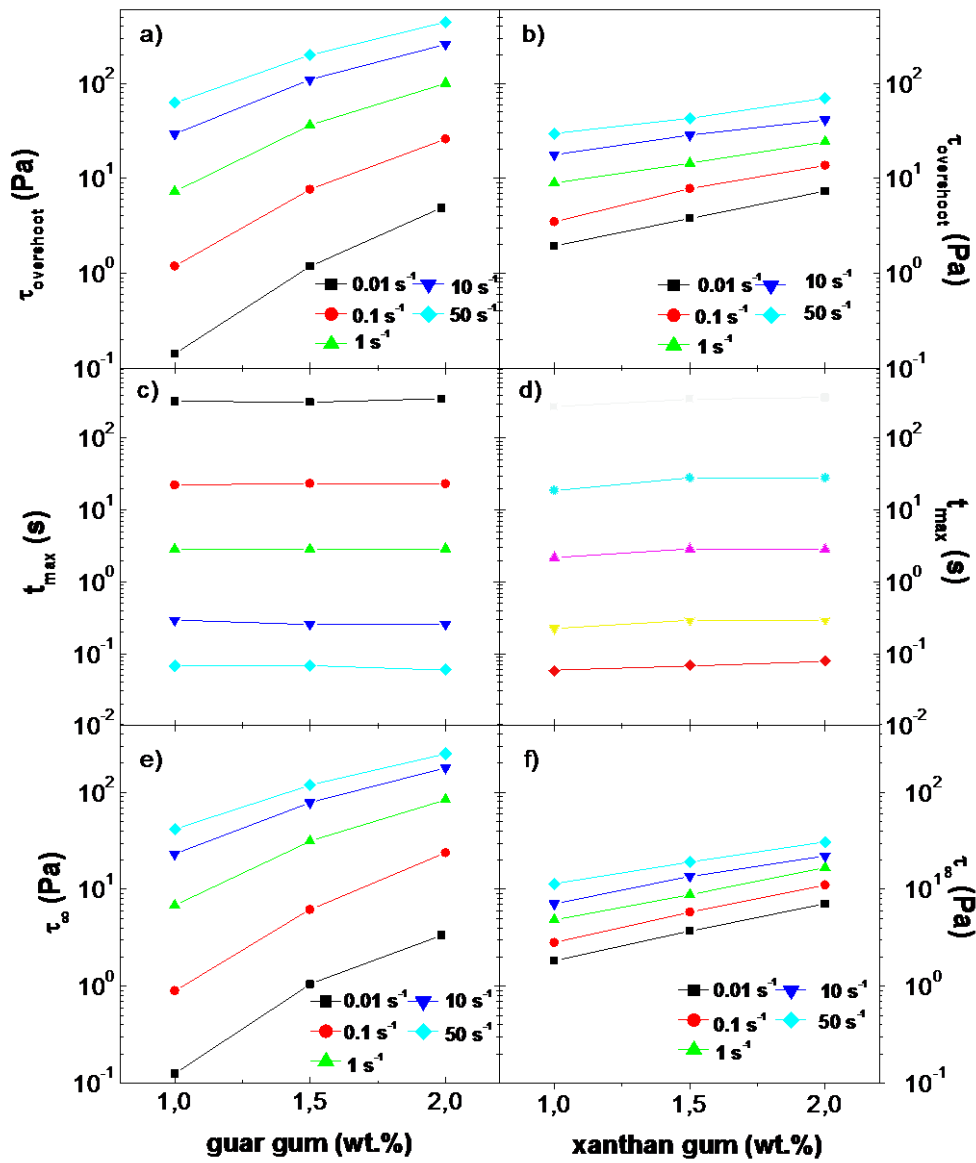
296 observed during stress growth experiments involve two opposite processes. The first
 297 part of these curves is mainly result of the well-known viscoelastic response, being the
 298 elastic deformation the prevailing component. This results in an almost linear increase
 299 of shear stress with time at the beginning, and an increasing non-linearity as shear time
 300 approaches the characteristic time defined by the stress overshoot. It is worth pointing
 301 out that the magnitudes of the stress overshoot seem to be strongly dependent on both
 302 the time and the shear rates applied to the sample (see **Fig. 5**). Once the stress overshoot
 303 is reached, the structural breakdown due to the shear flow process takes the main role.
 304 As a result, the shear stress, or the apparent viscosity, monotonically decreases in this
 305 region. This transient evolution continues until the steady state level is reached, which
 306 indicates that the time-dependent shear-induced microstructure become stable for the
 307 shear rate applied.



308

309 **Fig. 5.** Shear stress-growth curves, in a range of constant shear rates comprised between
310 0.01 and 50 s⁻¹, for selected aqueous gum solutions.

311 **Fig. 6** shows the values of some relevant characteristics parameters, derived from
312 analysis of stress grown curves, i.e., stress overshoot (τ_{\max}), equilibrium or steady-state
313 stress value (τ_{eq}), and elapsed time necessary to reach the stress overshoot for aqueous
314 gum solutions. As expected, the stress overshoot and the equilibrium shear stress
315 increased with the gum concentration. Guar gum solutions show higher stress overshoot
316 values than xanthan gum solutions at all shear rates, excepting the sample with lower
317 gum concentration. However, t_{\max} , which is related to the beginning of the structural
318 breakdown process, was larger for solutions containing xanthan gum. This implies that
319 xanthan gum solutions induces structural networks that are able to resist higher
320 deformations.



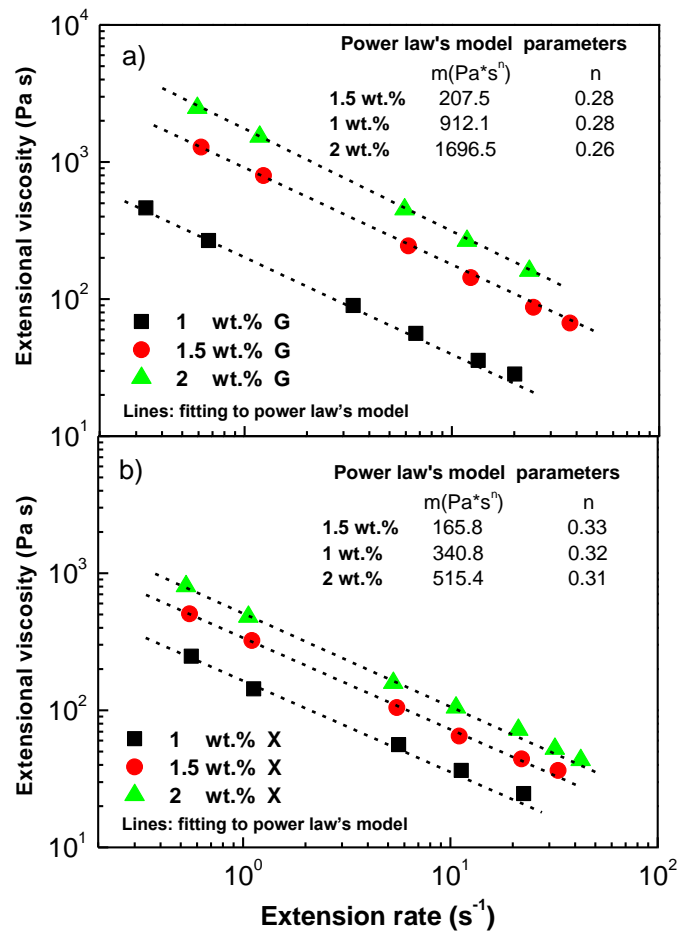
321

322 **Fig. 6.** Evolution of: a) the equilibrium shear stress, b) the stress overshoot, c) the time
 323 for the overshoot and d) the amount of overshoot, as function of gum content.

324 *3.4. Extensional flow*

325 The extensional viscosity for the different gum solutions as a function of the strain rate
 326 are shown in **Fig. 7**. The extensional viscosity decreased with increasing extensional
 327 strain rate, and it also decreased with lower gum concentration. As can be observed,
 328 guar solutions present higher viscosity than xanthan solutions on the whole range of

329 extensional rate studied, similar results were found by shear rheology. These curves
330 give evidence of a clear extension thinning behavior, and they could be fitted by the
331 Power law model for both solutions. The results for both guar and xanthan solutions are
332 presented in **Fig. 7**. The flow index values for the extensional measurements, “n”, is
333 consistent irrespective of gum concentration unlike those obtained in shear. Trouton
334 ratio (η_e/η) estimates the departure of ratio of extensional to shear viscosity from its
335 Newtonian counterpart, which is 3 for the Newtonian fluids (Berta, Wiklund, Kotz, &
336 Stading, (2016). In this this case, this value were taken at reference of 5 s^{-1} , shear
337 rate/extensional strain rate since in the model it indicates the n coefficients are similar
338 for the extension and shear curves. Trouton ratio for guar solutions was about ~20 and
339 for xanthan solutions were about ~40, i.e. higher than 3 for all the solutions which
340 confirms the elastic nature of the samples. Similar results were found by Qazi et al.,
341 (2017) for commercial gum or starch-based thickeners and by Torres et al., (2014) for
342 natural giesekus fluids.



343

344 **Fig. 7.** The extensional viscosity as a function of the extensional strain rate for aqueous
 345 guar (a) and xanthan (b) solutions.

346 **4. Concluding remarks**

347 The shear and extensional rheology of aqueous solutions of guar and xanthan gum with
 348 concentrations has been studied over the range 1-3 wt.%. Preparations of solutions were
 349 followed through the evolution of torque with processing time by using the mixing
 350 rheometry technique. Different stages subsequently related to gum addition, solution
 351 and further blending can be distinguished. The increase in torque values is more gradual
 352 when using guar gum and these results reveal that the type of hydrocolloids exerts a
 353 great influence on the process rheokinetics and resulting rheological response. The
 354 critical shear strain for linear response increased with gum concentration and xanthan

355 gum solutions show a somewhat longer LVR compared to guar, indicating the network
356 is less prone to yielding. SAOS tests within the linear viscoelastic region showed that
357 xanthan gum solutions studied behaved as a weak gel, whereas guar gum solutions
358 suggest the presence of entanglement and the formation of an elastic, gel-like structure.
359 The viscoelastic moduli values of both solutions markedly increased with total
360 polysaccharide concentration, maintaining the shape of the mechanical spectra. All the
361 systems exhibited shear-thinning behaviour. Flow curves were fitted to the Cross and
362 Power law models and the fitting parameters values were depend of the gum
363 concentration. Guar gum solutions obeyed the Cox-Merz rule, although with a
364 divergence at high rates for the more concentrated solutions, while the Cox-Merz rule
365 was not followed throughout the xanthan gum concentrations studied. These results
366 indicated the occurrence of a more developed structure. Transient stress data with time
367 at different constant shear rates of solutions showed typically non-linear viscoelastic
368 response, with a shear stress overshoot during the first stages of flow followed by a
369 steady state. The overshoot and steady-state stresses increased with the gum
370 concentration, whereas the time at which the stress overshoot occurs is only lightly
371 affected by the gum content. The extensional flow curves determined by Hyperbolic
372 Contraction Flow showed extension thinning behavior. The Trouton ratios were an
373 order of magnitude higher than the lower limit for Newtonian fluid, likely due to the
374 elasticity induced by the polysaccharides.

375 **Acknowledgements**

376 J.E. Martín-Alfonso received a Postdoctoral Research Grant from “Ayudas para
377 estancias de investigación postdoctorales” Programme of Campus de Excelencia
378 Internacional Agroalimentario (ceiA3). The authors gratefully acknowledge their
379 financial support.

380 **References**

- 381 Abdulrahman, A., Alquraishi, & Fares, D., Alsewailam, (2012). Xanthan and guar
382 polymer solutions for water shut off in high salinity reservoirs. *Carbohydrate*
383 *Polymers* 88 (2012) 859– 863.
- 384 Anna, S.L., & McKinley, G.H. (2001). Elasto-capillary thinning and breakup of
385 modelelastic liquids. *Journal of Rheology*, 45, 115.
- 386 Bach, A., Rasmussen, H., & Hassager, O. (2003). Extensional viscosity for polymer
387 melts measured in the filament stretching rheometer. *Journal of Rheology*, 47, 429-
388 441.
- 389 Berta, M., Gmoser, R., Krona, A. & Stading, M. (2015). Effect of viscoelasticity on
390 foam development in zeine starch dough. *LWT - Food Science and Technology*, 63,
391 1229-1235.
- 392 Berta, M., Muskens, E., Schuster, E. & Stading, M. (2016). Rheology of natural and
393 imitation mozzarella cheese at conditions relevant to pizza baking. *International*
394 *Dairy Journal*, 57, 34-38.
- 395 Berta, M., Wiklund, J., Kotz, R. & Stading, M. (2016). Correlation between in-line
396 measurements of tomato ketchup shear viscosity and extensional viscosity. *Journal*
397 *of Food Engineering*, 173, 8-14.
- 398 Binding, D.M., (1988). An approximate analysis for contraction and converging flows.
399 *Journal of Non-Newtonian Fluid Mechanics*, 27, 173-189.
- 400 Carmona, J.A., Ramírez, P., Calero, N. & Muñoz, J. (2014). Large amplitude oscillatory
401 shear of xanthan gum solutions. Effect of sodium chloride (NaCl) concentration.
402 *Journal of Food Engineering*, 126, 165–172.

- 403 Carmona, J.A., Lucas, A., Ramírez, P., Calero, N. & Muñoz, J. (2015). Nonlinear and
404 linear viscoelastic properties of a novel type of xanthan gum with industrial
405 applications. *Rheologica Acta*, 54, 993–1001.
- 406 Cox, W.P., & Merz, E.H. (1958). Correlation of dynamic and steady flow viscosities.
407 *Journal of Polymer Science*, 28, 619-622.
- 408 Cheng, Y., & Prud'homme, R.K. (2000). Enzymatic degradation of guar and substituted
409 guar galactomannans. *Biomacromolecules*, 1, 782–788.
- 410 Chenlo, F., Moreira, R. & Silva, C. (2010). Rheological properties of aqueous
411 dispersions of tragacanth and guar gums at different concentrations. *Journal of*
412 *Texture Studies*, 41, 396-415.
- 413 Choi, H., Mitchell, J.R., Gaddipati, S.R., Hill, S.E. & Wolf, B. (2014). Shear rheology
414 and filament stretching behaviour of xanthan gum and carboxymethyl cellulose
415 solution in presence of saliva. *Food Hydrocolloids*, 40, 71-75.
- 416 Choi, H.M. & Yoo, B. (2009). Steady and dynamic shear rheology of sweet potato
417 starch–xanthan gum mixtures. *Food Chemistry*, 116, 638–643.
- 418 Choppe, E., Puaud, F., Nicolai, T. & Benyahia, L. (2010). Rheology of xanthan
419 solutions as a function of temperature, concentration and ionic strength.
420 *Carbohydrate Polymers*, 82, 1228-1235.
- 421 Duxenneuner, M.R., Fischer, P., Windhab, E.J., & Cooper-White, J.J. (2008).
422 Extensional properties of hydroxypropyl ether guar gum solutions.
423 *Biomacromolecules*, 9, 2989-2996.
- 424 Entov, V.M., & Yarin, A.L. (1984). Influence of elastic stresses in the capillary breakup
425 of dilute polymer solutions. *Fluid Dynamics*, 19, 21–29.

426 Hasegawa, A., Ootoguro, A., Kumagai, H., & Nakazawa, F. (2005). Velocity of
427 swallowed gel food in the pharynx by ultrasonic method. *Journal of The Japanese*
428 *Society for Food Science and Technology-nippon Shokuhin Kagaku Kogaku Kaishi*,
429 52, 441-447.

430 Köpplmayr, T., Luger, H.J., Burzic, I., Battisti, M.G., Perko, L., Friesenbichler, W., &
431 Miethlinger, J. (2016). A novel online rheometer for elongational viscosity
432 measurement of polymer melts. *Polymer Testing*, 50, 208-215.

433 Lapasin, R., & Prici, S. (1995). Rheology of industrial polysaccharides: Theory and
434 applications. Glasgow: Blackie Academic and Professional.

435 Martín-Alfonso J.E. & Franco J.M. (2014). Ethylene-vinyl acetate copolymer
436 (EVA)/sunflower vegetable oil polymer gels: Influence of vinyl acetate content.
437 *Polymer Testing*, 37, 78–85.

438 Meissner, J. (1972). Development of a universal extensional rheometer for the uniaxial
439 extension of polymer melts. *Transactions of The Society of Rheology*, 16, 405-420.

440 Miquelim, J.N., & Lannes, S.C.D.S. (2009). Egg albumin and guar gum influence on
441 foam thixotropy. *Journal of Texture Studies*, 40, 623-636.

442 Moberg, T., Rigdahl, M., Stading, M., & Bragd E.L. (2014). Extensional viscosity of
443 microfibrillated cellulose suspensions. *Carbohydrate Polymers*, 102, 409–412.

444 Mudgil, D., Barak, S. & Khatkar, B.S. (2012). Effect of enzymatic depolymerization on
445 physicochemical and rheological properties of guar gum. *Carbohydrate Polymers*,
446 90, 224–228.

447 Münstedt, H., (1979). New universal extensional rheometer for polymer melts.
448 Measurement on a PS sample. *Journal of Rheology*, 23, 421-436.

449 Nystrom, M. (2015). Extensional rheometry through hyperbolic contraction (Ph.D.
450 thesis). Goteborg, Sweden: Chalmers University of Technology.

451 Nyström, M., Muhammad, W., Bülow, M., Ekberg, O., & Stading, M. (2015). Effects of
452 rheological factors on perceived ease of swallowing. *Applied. Rheology*, *25*, 63876-
453 63885.

454 Oom, A., Pettersson, A., Taylor, J.R.N. & Stading, M. (2008). Rheological properties of
455 kafirin and zein prolamins. *Journal of Cereal Science*, *47*, 109–116.

456 Piermaría, J., Bengoechea, C., Abraham, A.G., & Guerrero, A. (2016). Shear and
457 extensional properties of kefiran. *Carbohydrate Polymers*, *152*, 97–104.

458 Qazi, W.M., Wiklund, J., Altskär, A., Ekberg, O. & Stading, M. (2017). Shear and
459 extensional rheology of commercial thickeners used for dysphagia management.
460 *Journal of Texture Studies*. DOI: 10.1111/jtxs.12264.

461 Salinas-Vázquez, M., Vicente, W., Brito-de la Fuente, E., Gallegos, C., Márquez, J., &
462 Ascanio, G. (2014). Early numerical studies on the peristaltic flow through the
463 pharynx. *Journal of Texture Studies*, *45*, 155-163.

464 Sittikijyothin, W., Torres, D., & Gonçalves, M.P. (2005). Modelling the rheological
465 behaviour of galactomannan aqueous solutions. *Carbohydrate Polymers*, *59*, 339-
466 350.

467 Sridhar, T., Tirtaatmadja, V., Nguyen, D.A., & Gupta, R.K. (1991). Measurement of
468 extensional viscosity of polymer solutions. *Journal of Non-Newtonian Fluid
469 Mechanics*, *40*, 271–280.

470 Stading, M. & Bohlin, L. (2001). Contraction flow measurements of extensional
471 properties. *Transation Nordic Rheology Society*, *8/9*, 181-185.

472 Sworn, G. (2000). Xanthan gum. In G. O. Phillips & P. A. Williams (Eds.), Handbook
473 of hydrocolloids (pp. 103–115). Cambridge, UK: Woodhead Publishing Limited

474 Szopinski, D. & Luinstra, G.A. (2016). Viscoelastic properties of aqueous guar gum
475 derivative solutions under large amplitude oscillatory shear (LAOS). *Carbohydrate*
476 *Polymers*, 153, 312–319.

477 Tako, M., & Nakamura, S. (1985). Synergistic interaction between xanthan and guar
478 gum. *Carbohydrate Research*, 138, 207–213.

479 Tombs, M.P. & Harding, S.E. (1998). An introduction to polysaccharide biotechnology.
480 London: Taylor & Francis Ltd.

481 Torres, M.D., Hallmark, B., & Wilson, D.I. (2014). Effect of concentration on shear and
482 extensional rheology of guar gum solutions. *Food Hydrocolloids*, 40, 85-95.

483 Torres, M.D., Hallmark, B., Wilson, D.I. & Hilliou, L. (2014). Natural Giesekus fluids:
484 shear and extensional behaviour of food gum solutions in the semidilute regime.
485 *Aiche Journal*, 60, 3902-3915.

486 Wikstrom, K., & Bohlin, L. (1999). Extensional flow studies of wheat flour dough. I.
487 Experimental method for measurements in contraction flow geometry and
488 application to flours varying in breadmaking performance. *Journal of Cereal*
489 *Science*, 29, 217-226.

490